

Design and Control of Microgrid Fed by Renewable Energy Generating Source

Mr. Kunal Badhe¹, Mr. Kunal Gunjal², Mr. Shriprasad Gawande³, Mr. Anuroop Jadhav⁴
Mr. Vishwajeet Solanke⁵, Mr. Vaibhav Wankhede⁶

Students, Bachelor of Electrical Engineering^{1,2,3,4,5,6}
Shri Sant Gajanan Maharaj College of Engineering, Shegaon, India

Abstract: This study describes the control of a micro-grid in an isolated area that is powered by wind and solar hybrid energy sources. The wind energy conversion machine is a doubly fed induction generator (DFIG), and a battery bank is linked to a common DC bus of them. A solar photovoltaic (PV) array is utilised to convert solar power that is evacuated at the DFIG's common DC bus utilising a DC-DC boost converter in an efficient manner. The voltage and frequency are regulated via the line side converter's indirect vector control, which incorporates droop characteristics. It modifies the frequency set point based on the battery's energy level, which slows down overcharging or discharging. The system may also function when wind power is unavailable. Maximum power point tracking (MPPT) is a control technique used by both wind and solar energy blocks. The system is intended for fully autonomous functioning while taking into account all realistic situations. The system also has a facility for external power supply for battery charging, which is not required. In the Matlab environment, a simulation model of the system is created, and simulation results are shown under various scenarios such as unavailability of wind or solar energy, unbalanced and nonlinear loads, and low battery state of charge. Finally, a system prototype is built utilising a 5 kW solar PV array simulator and a 3.7 kW wrapped rotor induction machine.

Keywords: micro-grid

I. INTRODUCTION

There are numerous rural areas across the world that do not have access to energy. There are also numerous sites that are linked to the grid, but do not receive energy for up to 10-12 hours every day, causing residents' economic activities to suffer. Many of these locations are abundant in renewable energy (RE) sources such as wind, sun, and bio-mass. An autonomous generating system based on locally accessible renewable energy sources can significantly reduce reliance on grid electricity, which is mostly based on fossil fuels. Wind and solar energy sources are preferred over bio-mass-based systems since the latter is vulnerable to supply chain issues. Wind and solar energy, on the other hand, suffer from a high level of power fluctuation, a poor capacity utilisation factor, and an unpredictable nature. As a result of these considerations, solid power for autonomous systems cannot be ensured. While battery energy storage (BES) can assist reduce power fluctuations and boost predictability, the utilisation factor can be increased by running each energy source at its optimal operating point. The optimal operating point, also known as maximum power point tracking (MPPT), necessitates the management of the operating point of the wind energy generator and solar PV (Photovoltaic) array in terms of speed and voltage in order to collect the most electrical energy from the input resource. Power electronics (PE)-based control can be used to accomplish MPPT. PE-based control can also aid with BES energy management.

II. LITERATURE REVIEW

H. Zhu, D. Zhang, H. S. Athab, B. Wu, and Y. Gu[1] offer a photovoltaic (PV)-based stand-alone power system that is typically used to manage energy provided from several power sources, such as PV solar arrays and batteries, and supply continuous power to consumers in an appropriate manner. Three distinct dc/dc converters would have been utilised in the past. An integrated solution of PV isolated dc/dc three-port converter (TPC) is offered to cut costs and enhance power density of the power system. To enhance efficiency, all main diodes and MOSFETs can be switched to zero

current, and a continuous input current of the solar array is maintained by adding a magnetic switch produced from a fourth winding of the half-bridge transformer. The control techniques for the single module to realise maximum power point tracking (MPPT), battery charge control, and main bus regulation are presented based on the energy-balancing component produced by boost. The power system control mechanism for many modules in parallel is also devised, and the TPC power system may automatically switch between conductance mode and MPPT mode.

M. Das and V. Agarwal[2] offer a revolutionary three stand-alone solar photovoltaic (PV) system design that employs high-gain, high-efficiency (96%) dc-dc converters in both the forward power stage and the bidirectional battery interface. High-voltage gain converters enable the utilisation of low-voltage PV and battery sources. As a result, partial shadowing and parasitic capacitance effects on the PV source are reduced. The series connection of a high number of battery modules is avoided, eliminating overcharging and deep draining difficulties that diminish battery life. Furthermore, the suggested arrangement allows for "required power tracking (RPT)" of the PV source based on load needs, reducing the need for expensive and "difficult to manage" dump loads. High-performance inverter operation is obtained by abc to dq reference frame translation, which aids in producing exact information about the active power component of the load for RPT, ac output voltage management, and control complexity reduction. The modulation index of sinusoidal pulse width modulation is used to manage the inverter output voltage, resulting in stable and dependable system performance.

A. B. Ataji, Y. Miura, T. Ise, and H. Tanaka[3] offer a control method for a stand-alone doubly fed induction generator (DFIG) that is generally based on "sensorless" direct voltage control. It uses direct voltage management and negative-sequence correction through rotor-side converter to support asymmetric "unbalanced" loads. It highlights the restriction of the standard direct voltage control in obtaining the slip angle, and hence the limitation of the negative-sequence compensation control in supporting the complete range of asymmetric loads. To circumvent these restrictions, it provides a novel estimator of the angle of the rotor current in the synchronous reference frame. The proposed estimator requires just one DFIG parameter, stator inductance, which may be determined using real machine parameters. N.A. Orlando, M. Liserre, R.A. Mastromauro, and A. Dell'Aquila[4] describe the field of wind energy generation, with a concentration on distributed generation via tiny wind turbines (power unit 200 kW) due to their compact size and lesser environmental effect. The usage of asynchronous generators directly connected to the grid dominated the area of small generation until recently, when permanent magnet synchronous generators (PMSG) with power converters, either partially or completely regulated, became popular. It goes on the following control issues for small wind turbine systems: generator torque control, speed/position estimate, pitch control, brake chopper control, dc/dc converter control, and grid converter control. Specific challenges for tiny wind turbines occur in the optimisation and limiting of wind energy extraction, as well as in the creative idea.

III. MOTIVATION

Reduced carbon footprint of the community or organisation can be a driving force behind the design and management of a microgrid powered by renewable energy sources. Utilising clean, renewable energy sources helps cut down on greenhouse gas emissions, which are a factor in climate change.

IV. OBJECTIVE

The goal of planning and managing a microgrid powered by renewable energy sources is to provide a self-sufficient energy system that is affordable, dependable, efficient, and sustainable while lowering the community's or organization's carbon impact.

V. METHODOLOGY OF PROPOSED SYSTEM

The process for planning and managing a microgrid that is powered by renewable energy resources entails assessing the energy demand and available renewable energy sources, designing the microgrid and control system, doing simulations and tests, putting the system in place, and keeping it up and running over time. This strategy guarantees that the microgrid satisfies the energy demand and is cost-effective, efficient, and sustainable.

VI. SYSTEM COMPONENTS DESCRIPTION

Figure 1 depicts a single line schematic of the planned renewable energy generating system (REGS) fed micro-grid. The same has been constructed for optimum visibility. 15 kW power demand and 5 kW average power demand, respectively. In REGS, the rated capacity of both the wind and solar energy blocks is assumed to be 15 kW. Both energy blocks have a capacity utilisation factor of 20%, which is sufficient to provide the hamlet's full-day energy needs.

In the event of inadequate wind speed, the wind energy source is separated from the network using a 3-pole breaker, as indicated in the schematic figure. The battery bank connects the DC sides of both RSC and LSC, as well as the HV side of the solar converter. RSC assists the wind energy system in operating at the optimum rotation speed required by the W-MPPT algorithm. The voltage and frequency of the network are controlled by the LSC. Figure 2 depicts the system's energy flow diagram.

The following sub-sections demonstrate the design technique of important components of REGS.

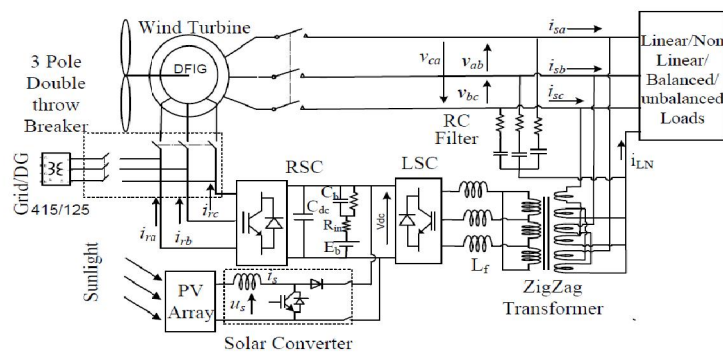


Fig.1 Schematic of isolated micro-grid network fed by renewable energy source using battery storage.

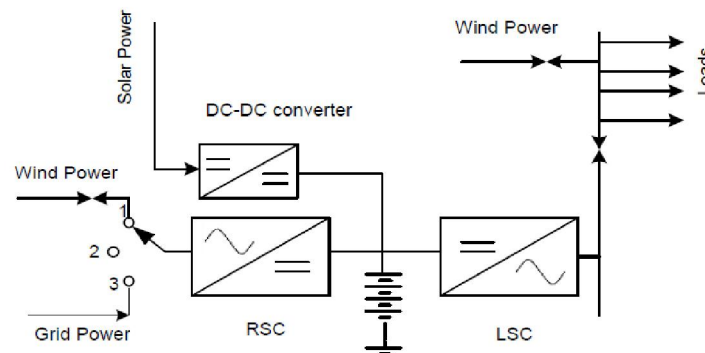


Fig.2 Energy flow diagram of isolated micro-grid network fed by renewable energy source using battery storage.

The wind turbine catches the kinetic energy of the wind and converts it into driving torque for DFIG. RSC supplies the whole magnetizing power needs of the machine when the wind turbine is in operation. Hence DFIG's 11.83 kW capacity is sufficient to transfer mechanical power from a 15 kW wind energy system to electrical energy. The load and stator terminals are linked to the LSC through a zig-zag transformer, which also serves as a neutral for single-phase loads on the 415 V side. The highest absolute value of rotor slip is 0.3, hence the maximum rotor voltage V_{rmax} is 125 V (0.3415 V). The voltage on the LV side of the zig-zag transformer is also set to V_{rmax} . As a result, the transformer's voltage ratio is 415/125 V, and its HV windings are linked to the stator and the load. The combined kVA demand of load and attached filters should be met by the zig-zag transformer. As a result, a 20 kVA transformer is selected to transmit rated power while also fulfilling the reactive power requirements of the linked loads and filters at peak demand.

The machine's maximum operational slip is 0.3. This slip corresponds to a DFIG speed of 110 rad/s. The line voltage of the rotor V_{rmax} becomes 125 V (4150.3) at this slip. VL is the greater of the line voltage on the zig-zag transformer's low voltage (LV) side and the rotor voltage at maximum slip. The maximum working slip is 0.3, and the maximum

rotor voltage as well as the LV side of the zig-zag transformer is 125 V. The modulation index, m_i , is set to one. Based on these inputs, the DC bus voltage V_{dc} required for PWM control operation cannot be less than 204 V. V_{dc} is set to 240 V in the system shown. The proposed micro-grid is intended to meet a load requirement of 5 kW without the need of a generating source for up to 12 hours. Taking a 20% cushion for energy losses during energy exchange, the needed battery storage capacity is 72 kWh. At 240 V DC bus voltage, the battery's Ampere-Hour (AH) rating is 300 AH (72,000/240). This is accomplished by dividing 40 12V, 150 AH lead acid batteries into two parallel circuits.

VII. SYSTEM MODELING

The wind turbine catches the kinetic energy of the wind and converts it into driving torque for DFIG. RSC supplies the whole magnetizing power needs of the machine when the wind turbine is in operation. Hence DFIG's 11.83 kW capacity is sufficient to transfer mechanical power from a 15 kW wind energy system to electrical energy. The load and stator terminals are linked to the LSC through a zig-zag transformer, which also serves as a neutral for single-phase loads on the 415 V side. The highest absolute value of rotor slip is 0.3, hence the maximum rotor voltage V_{rmax} is 125 V (0.3415 V). The voltage on the LV side of the zig-zag transformer is also set to V_{rmax} . As a result, the transformer's voltage ratio is 415/125 V, and its HV windings are linked to the stator and the load. The combined kVA demand of load and attached filters should be met by the zig-zag transformer. As a result, a 20 kVA transformer is selected to transmit rated power while also fulfilling the reactive power requirements of the linked loads and filters at peak demand.

The machine's maximum operational slip is 0.3. This slip corresponds to a DFIG speed of 110 rad/s. The line voltage of the rotor V_{rmax} becomes 125 V (4150.3) at this slip. V_L is the greater of the line voltage on the zig-zag transformer's low voltage (LV) side and the rotor voltage at maximum slip. The maximum working slip is 0.3, and the maximum rotor voltage as well as the LV side of the zig-zag transformer is 125 V. The modulation index, m_i , is set to one. Based on these inputs, the DC bus voltage V_{dc} required for PWM control operation cannot be less than 204 V. V_{dc} is set to 240 V in the system shown. The proposed micro-grid is intended to meet a load requirement of 5 kW without the need of a generating source for up to 12 hours. Taking a 20% cushion for energy losses during energy exchange, the needed battery storage capacity is 72 kWh. At 240 V DC bus voltage, the battery's Ampere-Hour (AH) rating is 300 AH (72,000/240). This is accomplished by dividing 40 12V, 150 AH lead acid batteries into two parallel circuits.

A lead acid battery bank may be safely operated at voltages ranging from 2.25 V to 1.8 V per cell. As a result, the maximum and minimum battery voltages V_{bmax} and V_{bmin} are 270 V and 216 V, respectively. A battery bank can be imagined to be a direct current source with a fictional capacitor C_b and an internal resistance R_{in} linked in series. In addition, another resistance R_b is connected across the battery to represent energy depletion caused by self-discharge. The solar cell is the fundamental component of a solar PV system. The solar panels are set up so that the open circuit voltage of the solar string is less than the lowest downstream voltage of the solar converter or the DC bus voltage, V_{dc} . V_{occ} is calculated as 0.64 V based on average commercially available cell properties and its value. According to subsection (D), the minimum battery voltage can drop as low as 216 V. The solar array voltage (u_s) might fluctuate by up to 3% owing to module manufacturing tolerances. As a result, V_{dcm} is assumed to be 210 V, and the needed number of cells, N_c , is 328 cells. 324 cells are used to uniformly distribute the cells in a conventional arrangement, which are grouped into 9 modules of 36 cells each. For a typical module characteristic, the ratio of V_{occ} to cell voltage at maximum power point (MPP), V_{mpc} is 1.223. As a result, the module voltage at MPP is ($V_{mpc} \times 36$) 18.83 V and u_s is 169.47 V. At MPP, the total string current at 15 kW solar array capacity is 15000/(9*18.83)88.5 A. The number of strings in the solar array is set to 11, therefore the module current at MPP, I_{mp} is 8.04 A. For a typical module, the ratio of short circuit current I_{sc} to I_{mp} is 1.081, hence I_{sc} is 8.69 A. To eliminate voltage ripples, a high pass filter with a time constant smaller than the fundamental frequency, i.e. 20 ms, is employed at the stator terminal.

VII. CONTROL ALGORITHM

REGS, as illustrated in Fig.1, is made up of three converters, the descriptions of which are as follows.

Control of Solar Converter:

A solar converter is a boost-type DC-DC converter that uses incorporated S-MPPT electronics to evacuate solar the solar system performs at MPP. Figure 3 depicts the flow diagram of the MPPT algorithm.

Control of LSC:

Because onshore wind turbines generate power only 60-70% of the time, the system should be built to function even when there is no wind. i_{qs}^* has two components, as shown in the control diagram in Fig. 4. When a wind turbine is operational, the first component, i_{qs1} , corresponds to the power component of DFIG current. The second component, i_{qs2} , represents the power component pulled while the DFIG stator is not attached to the load terminal.

VIII. MATLAB SIMULINK

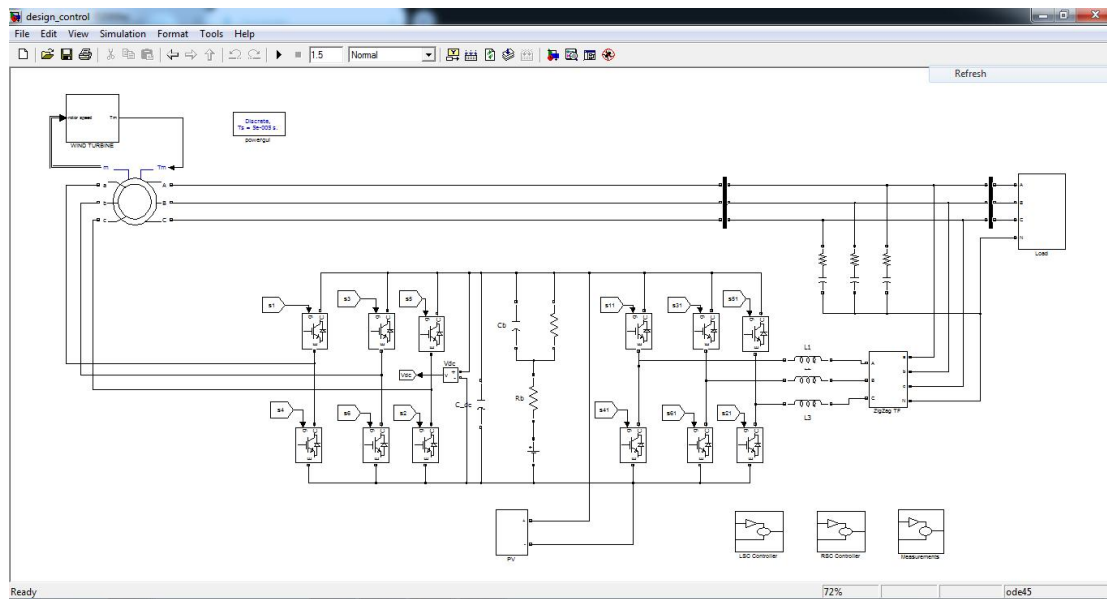


Fig.3 Matlab Simulation

VIII. FUTURE SCOPE

Future advancements in energy storage, the incorporation of artificial intelligence and machine learning, the development of common standards for interoperability, the electrification of transportation, and energy trading via blockchain technology could all be included in the Design and Control of Microgrid Fed by Renewable Energy Generating Source.

Improving the duration of flight time by boosting the battery's size.

These advancements may improve the performance and stability of microgrids, provide new revenue streams, and aid in the transition to renewable energy and decentralized energy systems.

IX. RESULT AND DISCUSSION

MATLAB is used to create the Simulink model of a microgrid supplied by REGS. The functionalities of the solar panels and wind turbines are modelled.

Figure 4 depicts the system's performance when the wind generator is added and removed.

Figure 5 depicts the system's performance when the solar PV system is added to and removed from the system. Both of the above examples go over MPPT operation through RSC and solar converter.

Figure 6 depicts results at loss of load and Fig. 7 at unbalanced nonlinear load

Figure 8 depicts a scenario in which stored energy and generated power is low and external charging through RSC is required.

Figure 9 depicts a scenario in which the DC bus voltage is set to high charging power

Performance of System at Constant Load and Cut-in and Cut-out of Wind Power:

The system is started with 10 kW and 6kVAR load without wind or solar energy sources, as illustrated in Fig. 6.1.1. The wind generator is turned on at $t=0.25$ s with a wind speed of 7 m/s. As a result, there is a brief fluctuation in the system voltage. The wind speed of the turbine is increased from 7 m/s to 8 m/s at $t=0.6$ s, then reduced to its original value at $t=0.1$ s. According to the W-MPPT algorithm, the rotor control action maintains the required rotational speed. The wind generator is turned off at $t=0.14$ s.

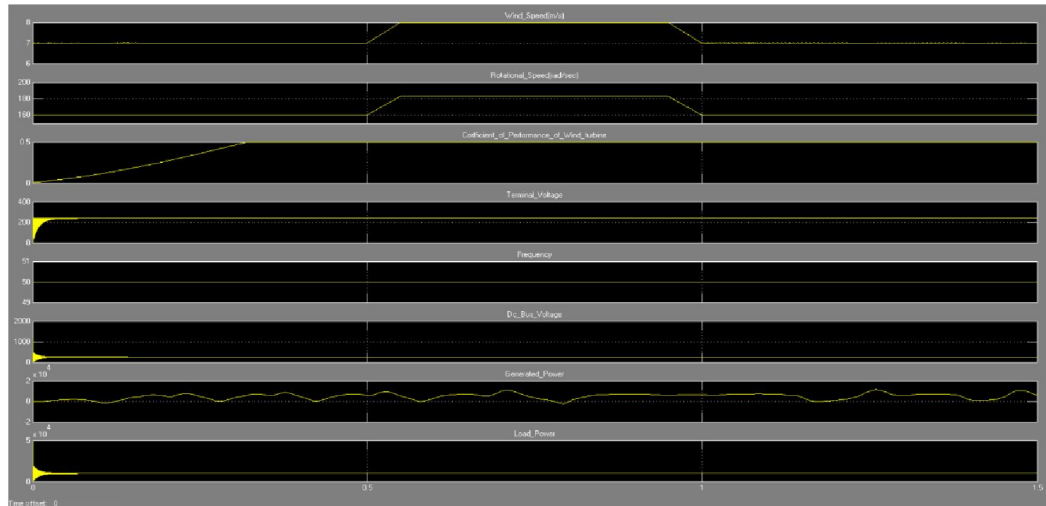


Fig.4

Performance of System at Constant Load and Cut-in and Cut-out of Solar Power:

Without wind or solar energy, the system starts with a 10 kW and 6 kVAR load. As illustrated in Fig. 5, the solar system enters operation at $t=0.25$ s with a radiance of 800 W/m². Solar radiation is increased to 900 W/m² at $t=0.4$ s and then lowered to 800 W/m² at $t=0.6$ s. The solar converter regulates the voltage of the solar PV system and runs at S-MPPT. At $t=0.7$ s, the solar system is turned off. At any transition point, no substantial difference in system voltage is seen.

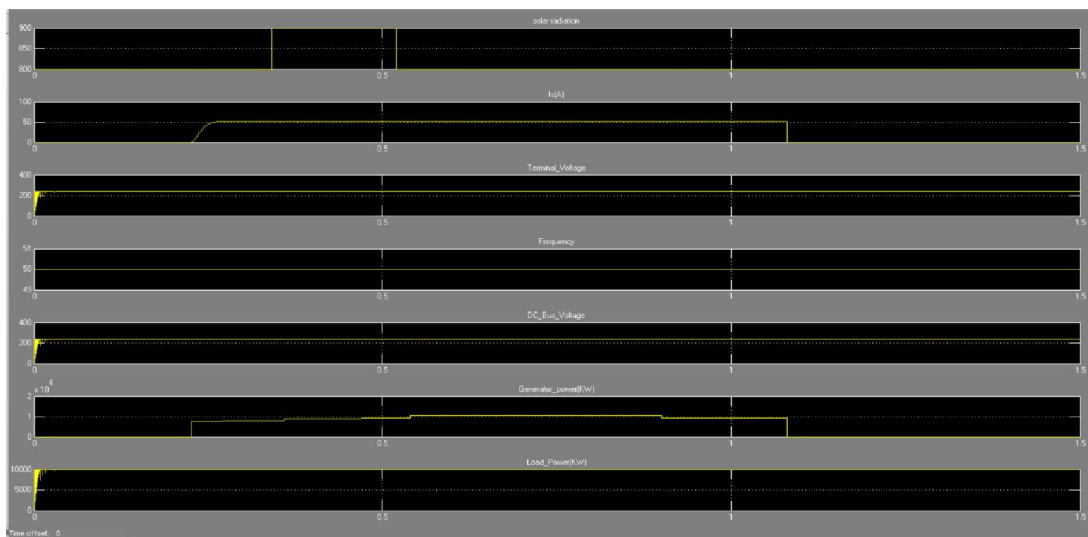


Fig.5

Performance of System at Unbalanced Nonlinear Load:

Figure 6 depicts the system's performance at imbalanced nonlinear. A microgrid should be appropriate for providing an imbalanced nonlinear load. When there are no producing sources, the worst-case scenario is used. The linked load

consists of a linear load of 2 kW and a nonlinear load of 8 kW. The a-phase load is removed from the network at $t=0.325$ s, followed by the b-phase load at $t=0.346$ s. The results show that the system can supply quality electricity to its customers even when the load is uneven or nonlinear

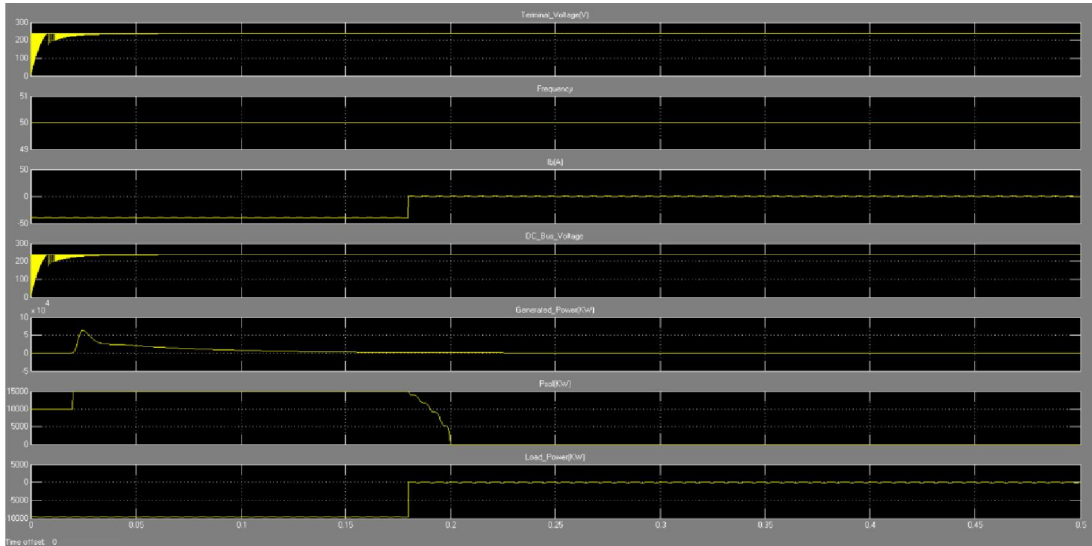


Fig.6

Performance of System at Loss Of load:

Figure 7 depicts the performance of the micro-grid in the event of a load loss. Prior to the commencement of the simulation, a 10 kW and 6 kVAR load is attached at the terminals. There is no wind or solar power, thus the load is powered by the battery. The system load is disconnected at $t=0.2$ s. It is discovered that the network's system voltage and frequency stay constant.

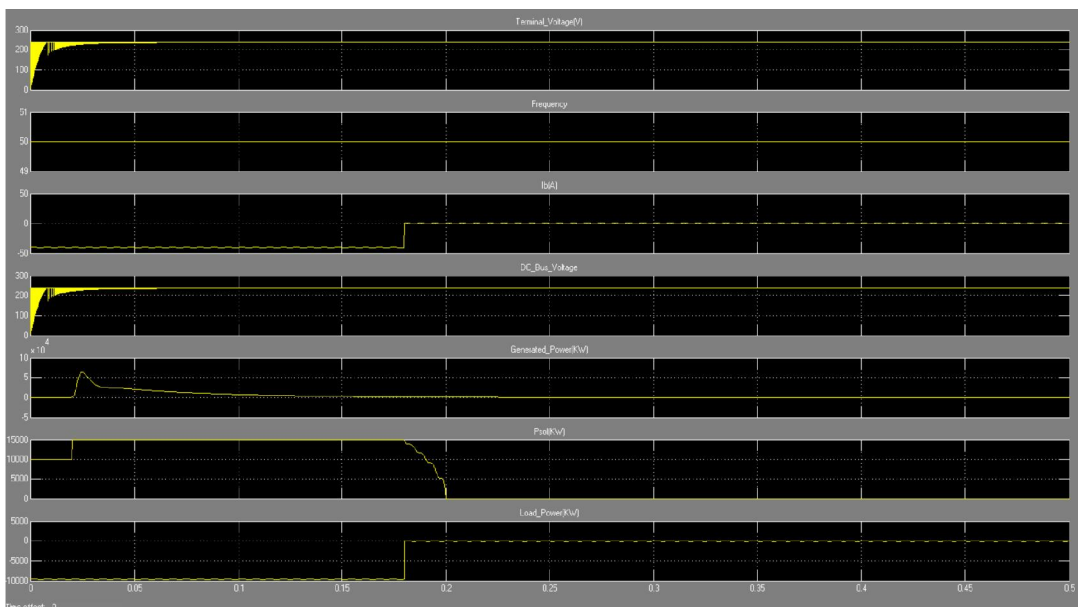


Fig.7

Performance of System at Unbalanced Nonlinear Load:

Figure 8 depicts the circumstance where there are no producing sources feeding the network and the battery is low. External charging is necessary to keep the load running. The charging circuit is activated based on the logic state. Wind production is turned off at $t=0.4$ s, and the charging circuit is activated due to decreasing battery voltage. As a consequence, external power is pumped via the RSC to meet load requirements while also charging the batteries.

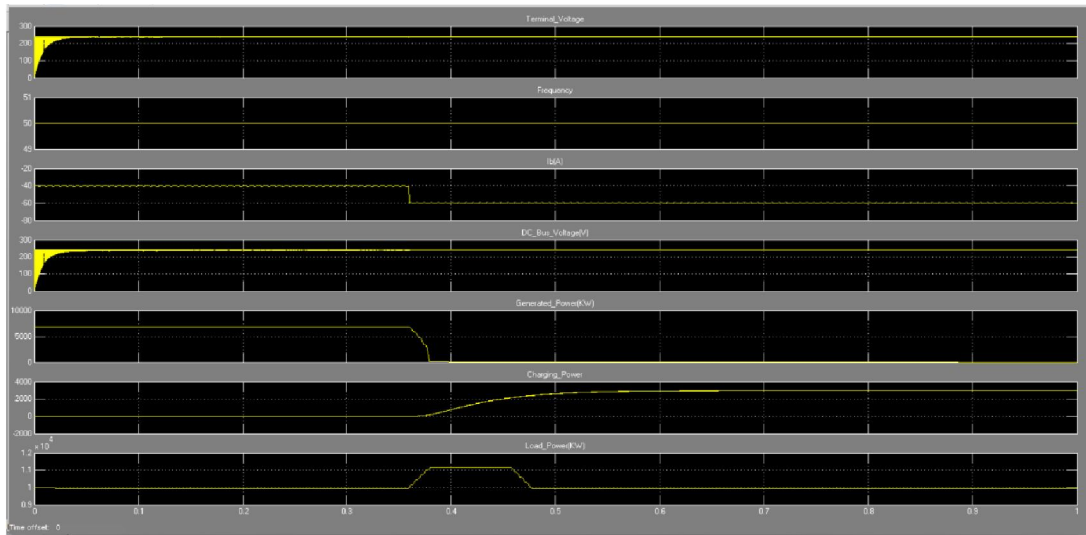


Fig.8

Performance of System during High Generation and Over-voltage Scenario of DC bus:

Figure 9 depicts the system's performance under high net generation and over-voltage scenarios of the DC bus. The AH of the battery is lowered by $1/200$ to make the effect obvious. Wind speed and sun irradiation are held constant at 9 m/s and 700 W/m², respectively. The graph shows that after the V_{dc} reaches 260 V, RSC control lowers the DFIG speed set point to 85% of the MPPT set point. Figure 5.12 shows that the charging power, P_c, and voltage increase are lowered.

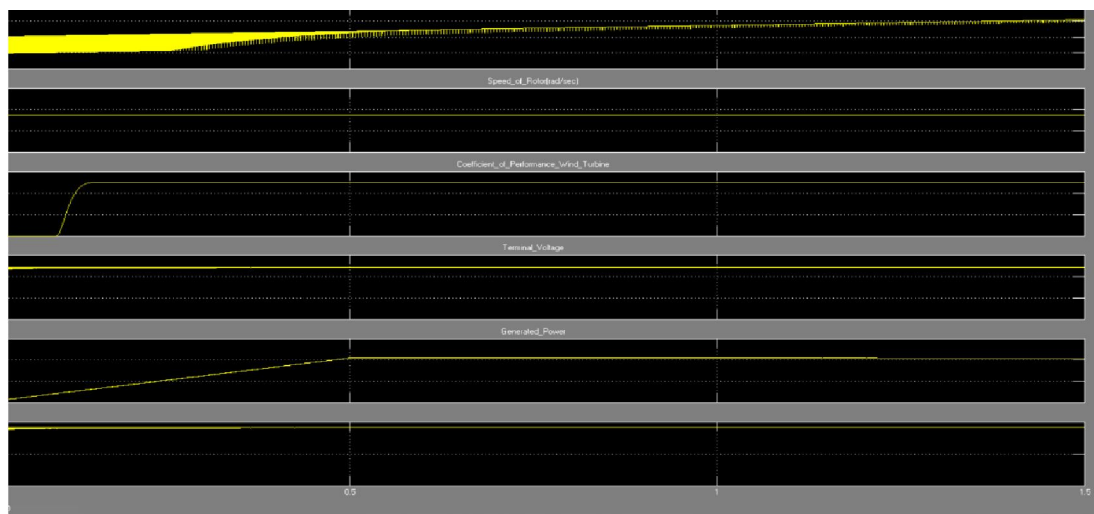


Fig.9

X. CONCLUSION

The proposed micro-grid system fed from REGS has been found suitable for meeting load requirement of a remote isolated location comprising few households. REGS comprises of wind and solar energy blocks, which are designed to extract the maximum power from the renewable energy sources and at the same time, it provides quality power to the consumers. The system has been designed for complete automated operation. This work also presents the sizing of the major components. The performance of the system has been presented for change in input conditions for different type of load profiles. Under all the conditions, the power quality at the load terminals, remains within acceptable limit. The effectiveness of the system is also presented with test results with prototype in the laboratory. The system has also envisaged the external battery charging by utilizing the rotor side converter and its sensors for achieving rectifier operation at unity power factor.

REFERENCES

- [1]. H. Zhu, D. Zhang, H. S. Athab, B. Wu and Y. Gu, "PV Isolated Three- Port Converter and Energy-Balancing Control Method for PV-Battery Power Supply Applications," *IEEE Transactions on Industrial Electronics*, vol. 62, no. 6, pp. 3595-3606, June 2015.
- [2]. M. Das and V. Agarwal, "Novel High-Performance Stand-Alone SolarPV System With High-Gain HighEfficiency DC-DC Converter PowerStages," *IEEE Transactions on Industry Applications*, vol. 51, no. 6, pp.4718-4728, Nov.-Dec. 2015.
- [3]. A. B. Ataji, Y. Miura, T. Ise and H. Tanaka, "Direct Voltage ControlWith Slip Angle Estimation to Extend theRange of SupportedAsymmetric Loads for Stand-Alone DFIG," *IEEE Transactions onPower Electronics*, vol. 31, no. 2, pp. 1015-1025, Feb. 2016.
- [4]. N.A. Orlando, M. Liserre, R.A. Mastromauro and A. Dell'Aquila, "Asurvey of control issues in PMSG-basedsmall wind turbine system,"*IEEE Trans. Industrial Informatics*, vol.9, no.3, pp 1211-1221, July2013.
- [5]. T. Hirose and H. Matsuo, "Standalone Hybrid Wind-Solar Power Generation System Applying Dump Power Control Without Dump Load," *IEEE Trans. Industrial Electronics*, vol. 59, no. 2, pp. 988-997, Feb. 2012.
- [6]. Z. Qi, "Coordinated Control for Independent Wind-Solar Hybrid Power System," 2012 Asia-Pacific Power and Energy Engineering Conference, Shanghai, 2012, pp. 1-4.
- [7]. S. K. Tiwari, B. Singh and P. K. Goel, "Design and control of autonomous wind-solar energy system with DFIG feeding 3-phase 4-wire network," 2015 Annual IEEE India Conference (INDICON), New Delhi, 2015, pp. 1-6.
- [8]. Emmanouil A. Bakirtzis and Charis Demoulias "Control of a micro-grid supplied by renewable energy sources and storage batteries,"*XXth Inter. Conf. on Electrical Machines (ICEM)*, pp. 2053-2059, 2-5 Sept. 2012.
- [9]. Z.M. Salameh, M.A. Casacca and W.A. Lynch, "A mathematical model for lead-acid batteries," *IEEE Trans. Energy Convers.*, vol. 7, no. 1, pp. 93-97, Mar.1992.
- [10]. A B. Rey-Boué, R García-Valverde, F de A. Ruz-Vila and José M. Torrelo-Ponce, "An integrative approach to the design methodology for 3-phase power conditioners in Photovoltaic Grid-Connected systems," *Energy Conversion and Management*, vol. 56, pp. 80-95, Dec 2011.
- [11]. H. Polinder, F. F. A. van der Pijl, G. J. de Vilder and P. Tavner, "Comparison of direct-drive and geared generator concepts for wind turbines," *IEEE International Conference on Electric Machines and Drives*, 2005., San Antonio, TX, 2005, pp. 543-550.
- [12]. S. K. Tiwari, B. Singh and P. K. Goel, "Design and control of micro-grid fed by renewable energy generating sources," 2016 IEEE 6th Inter. Conference on Power Systems (ICPS), New Delhi, 2016, pp. 1-6.